Indonesian Journal of Data and Science

Volume 6 Issue 3
ISSN 2715-9936
https://doi.org/10.56705/ijodas.v6i3.354

Research Article

Medium Range Meteorological Drought Prediction Based on SPEI-3 Using Ensemble Machine Learning and Deep Learning in North West Province, South Africa

Reatlegile Phiri [1,*]; Bukohwo Michael Esiefarienrhe [2]; Ibidun Christiana Obagbuwa [3]
[1] North-West University, Mahikeng, South Africa, phirireatlegile14@gmail.com
[2] North-West University, Mahikeng, South Africa, Michael.Esiefarienrhe@nwu.ac.za
[3] Walter Sisulu University, Mthatha, South Africa, iobagbuwa@wsu.ac.za

Correspondence should be addressed to Reatlegile Phiri: phirireatlegile14@gmail.com

Received 10 August 2025; Accepted 28 November 2025; Published 31 December 2025

Abstract:
Meteorological drought monitoring is a pivotal action in everyday humankinds' activities around the globe. It evaluates atmospheric conditions using weather observation instruments to measure atmospheric variables. Due to the highly sophisticated atmospheric environment, errors in drought monitoring and uncertain observation have been observed. Therefore, this research paper develops a lightweight Machine Learning (ML) and Deep Learning (DL) framework to forecast medium term meteorological drought in North West, South Africa using Standardized Precipitation Evapotranspiration Index at 3 -months (SPEI-3) timescale. This time scale reflects moisture deficits directly impacting agricultural production, early warning decisions and water management. The dataset used in this research study was obtained from South African Weather Services through a formal data request submission and not publicly accessible over a period of 10 years. Furthermore, the dataset consists of 20085 data entries and 11 data columns collected from 10 weather stations. The proposed models include SVR-RF, and, CNN-LSTM-ANN, compared to benchmark models, such as SVR, RF, CNN, LSTM, ANN, CNN-LSTM evaluated using statistical metrics, such as MSE, MAE, and r^2. The results demonstrated irregular drought patterns during the defined period with SPEI-3 values clustered below normal conditions. Similarly, validation results showed that SVR demonstrated strong predictive performance with competitive MSE of 0.28, low MAE of 0.34 and r^2 of 0.86. Although, the proposed CNN-LSTM-ANN and SVR-RF models did not exhibit competitive performance compared to benchmarking models, the result provides valuable comprehension, data collection, distribution, architecture, and computational power.

Keywords: Ensemble Machine Learning, meteorological drought prediction, Deep Learning, NWP, SPEI.

1. Introduction

Meteorological drought, is a prolonged and complex natural occurrence associated with evapotranspiration, influenced by fluctuation in climate conditions, substantially causing severer impact globally to the water management, drought emergency response and long term planning [1], [2], [3]. Intense meteorological drought propagates across domains, such as agriculture, hydrology, social economy causing drought stress; as atmospheric parameters; precipitation, temperature, evaporations impact ground water, soil moistures, water storage, etc. [1]. Accurate prediction of meteorological drought is an intricate temporal spatial endeavour, as meteorological parameters are highly sophisticated due to the complexity of the atmospheric and climate environment [2]. However,

various strategies are used to mitigate the adverse impacts caused by extreme meteorological drought, these include traditional water conservation, water storage, amongst others [4]. Moreover, technological approach includes the development of various indices, Numerical Weather Prediction (NWP), Artificial Intelligence (AI) based models (ML and DL) nested with drought indicators to improve forecasting and early warning capabilities. In the early 1990s, a Standardized Precipitation Index (SPI) was introduced and became a widely utilized drought index throughout the world in several research studies on drought prediction due to its simplicity in estimating dry or wet conditions using a single atmospheric parameter: precipitation. However, subsequent studies indicates that in semi-arid areas, SPI yields high uncertain results [3]. To address this limitation, researchers reformulated the SPI and proposed Standardized Precipitation Evapotranspiration Index (SPEI), an improved multiscale index that utilizes precipitation, and evapotranspiration as predictor parameters. The computational procedures of SPEI and SPI are similar; however, SPEI uses water balance, which is the difference between precipitation and evapotranspiration to compute drought severity. Other widely used indices (not limited to) include Palmer drought severity index (PDSI), Drought Area Index (DAI), Hutchinson Drought Severity index [1], [2], [3].

In recent years, statistical and dynamic approaches have been used to predict drought, and substantial research efforts have been dedicated to developing a more sustainable mechanism to accurately predict drought beyond empirical models considering the complexity of the atmospheric environment. In this regard, ML algorithms have made advances in drought prediction research demonstrating effectiveness in prediction accuracy and flexibility in processing complex non-linearity meteorological parameters [1], [3], [4], [5]. For example, Zhong *et al.* [6] utilized GenCast and SEEDS for ensemble operational Numerical Weather Prediction, in their study they argued that using ML model on deterministic forecasting have some limitation, hence they proposed an advanced ML model FuXI-ENS. On that note, Support Vector Regression (SVR), Linear Regression, Matern Gaussian Process Regression (Matern GPR) are novel model used in semi-arid area to forecasts drought, the authors of this study proposed bagging, hyperparameters, etc., techniques to improve the prediction accuracy of these algorithms' applied to SPI on various scales [7]. In contrast, DL rapidly gained traction in weather forecasting alternatively to physical based numeric models, statistical ensembles, and ML models. One study investigated the long-term daily temperature across stations in Ontario and Canada, the performance of DL models is remarkable with high relative accuracy [8], [9]. Yalçın *et al.*[10] proposed a hybrid DL approach, consisting of CNN and LSTM using SPEI base parameters to estimate drought for a 12 month time scale at four weather stations in Türkiye. Author in [11] investigated the integration of wavelets transformations and AI model in the Mun rivers basin, Thailand using Bootstrapped random forest (BRF), Bidirectional LSTM (Bi-LSTM), and a hybrid wavelet BRF, wavelet Bi-LSTM models over the period of 29 years' meteorological data. Wavelet BRF for SPI-3, 6, 12 demonstrated superior results compared to BRF, while wavelet Bi-LSTM outperformed Bi-LSTM. Other scholars explored Temporal convolutional networks (TCN) and LSTM, together with SR, SVR, and RF [12]. However, ML and DL models are data driven algorithms, typically requiring high quality data, with human interaction required for preprocessing, feature selection and model configuration.

Explicit demographic research gap is notable, where Africa is underrepresented, demonstrating a call for improved data collection, weather station infrastructure and data representation for diverse populations [13]. Several research scholars applied CNN-LSTM-ANN to study solar radiation predictions, soil moisture, however, there is a lack of studies utilizing the proposed algorithms for medium range forecast at this level of study [14], [15], [16], [17]. Therefore, this research study proposes a lightweight medium range forecast in the North West Province of South Africa using DL algorithms (CNN, LSTM, ANN) and Ensemble ML algorithms (SVR and RF) for SPEI 3-months to forecast drought impacts. To achieve the aim of this study, the following primary objective are followed: 1) Identify drought characteristics in the study area based on daily meteorological data from 2013 – 2023. 2) Develop a hybrid DL model and ensemble ML model that resemble SPEI. 3) Results comparison and best model chosen based on accurate predictions. These objectives advance meteorological drought forecasting through addressing specific challenges faced by the North West region by providing context-specific findings to enhance planning and decision-making. Furthermore, the proposed framework redefines and improves drought prediction methodologies. The structure of this article is as follows: Section 2 presents data collected and methods. In section 3, the study methodology is presented. Section 4 presents models performance and discussions. Lastly, section 5 presents the main findings and conclusion on the evaluation's models. **Figure 1** shows an overview of this study.

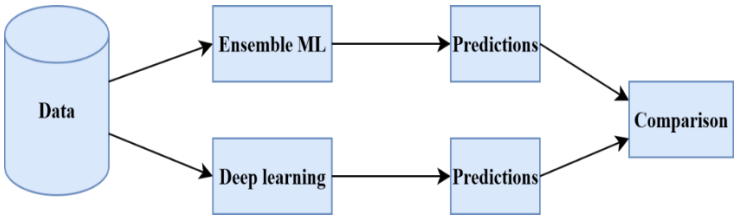

Figure 1. Study overview

2. Methods and Materials

In this section, a presentation on the study area, data collections, and methods used is made in each subsection.

Study Area:

This study focuses on the North West Province, which is in the northern part of South Africa, as shown in **Figure 2**. The area is 106 512 square kilometres span over 26.6639° S, 25.2838° E. The province is around the borders of Limpopo, Gauteng, Free State, Northern Cape provinces, and the neighbouring country of Botswana. Grassland and scattered trees make up the flat areas of the provinces. The south region consists of salt pans, while the west and northern parts are desert and bushveld, respectively. The province's climate during the summer period ranges between 22°and 34 °C, during winter, a single day records 2° to 20° C with an average of 16°C. This regions annual rainfall with precipitations is recorded to be about 360 and 500 mm respectively [18].

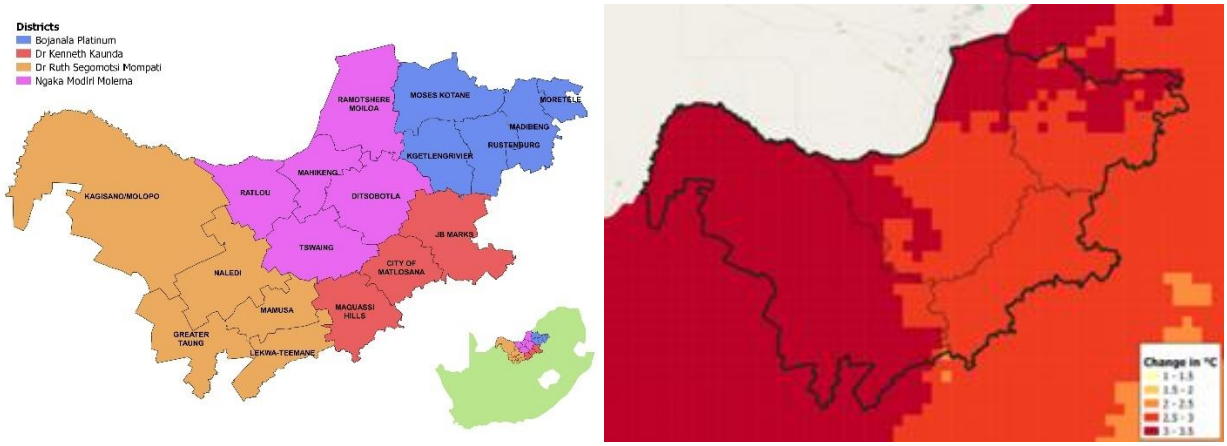

(a) (b)

Figure 2. (a) Geographic location of the study area, (b) Annual average temperature NW over the period 2021 – 2050 [19]

In 2015 and 2019, several reports indicated that the North West Province experienced a significant impact on agricultural, wildlife, and other sectors of the province due to prolonged drought. Outskirt places within the province, such as Disaneng, Tosca, and Taung, showed the impact of severe drought within communities in the southern region of Africa. Local Government Climate Change Support Program conducted a study using the RCP 8.5 scenario to highlight the severe increase in annual temperature throughout the province for the period 2021 – 2050. The findings of this study show that the province will be affected by extreme high temperatures that will have a significant impact on food and water security within the province in the coming years [19], [20], [21].

Data Collection:

Data was collected from a public weather forecasting agency called South African Weather Service, which collects and archive historical reliable, quality daily maximum temperatures, minimum temperatures, average temperatures, precipitation, snow, wind direction, wind speed, pressure, and other meteorological variable, across all weather stations within the North West Province over a period of 10 years from 1 January 2013 to 31 December 2023. 20085 data sample were collected from 10 weather stations in the region namely Mahikeng, Rustenburg, Potchefstroom,

Klerksdorp, Vryburg, Lichtenburg, Zeerust, Mafikeng Airport, Taung, and Brits. Although SAWS observes and records data using manual and automated systems, missing precipitation, average temperature, minimum, and maximum temperatures were observed in the data. However, appropriate statistical techniques were applied to handle affected entries with missing data, consequently, irrelevant columns were dropped leaving us with 8062 entries and 4 columns out of 11 columns, while evapotranspiration and SPEI were calculated and stored using Equations 1 and 3 respectively. To ensure the validity and adequacy of the data, the Bartlett test, Ljung-Box test, Autocorrelation Function, and Augmented Dickey-Fuller test were applied to determine homogeneity, independence, and stationarity across the variables in **Table 1**. The tests in Table 1 determined that the collected data is stationary, but autocorrelated with no erratic fluctuations with precipitation demonstrating heterogeneity between the variables. Data availability did not include financial conflicts.

Table 1. P-Value Test

Variable	Ljung-Box Test p-value	ADF p-value	Bartlett's Test p-value
T average	0.0	0.0	0.7630
T minimum	0.0	0.0	0.7462
T maximum	0.0	0.0	0.1318
Precipitation	3.35e-231	0.0	0.0006

Standard precipitation evapotranspiration index (SPEI):

SPEI is an extension of SPI that McKee proposed as an indicator considering precipitation data. However, as the years evolved, SPEI was invented to convey the deficiency shown by SPI. This index considers PET values and precipitation to monitor, evaluate, and express drought under various climate conditions. Although SPEI is the most frequently utilized index, research shows a possibility of sensitivity to various atmospheric conditions and time scales in different applications. The SPEI computation is initialized by calculating water balance (D_i), the difference between precipitation (P_i) and evapotranspiration (PET_i), then the difference is then normalized using the logarithmic probability function. However, PET_i is computed using a simple Hargreaves-Samani (HS) equation [1], [3], [5], [22], [23]:

$$PET\ (\text{mm} \cdot \text{day} - 1) = 0.0023(T_{max} - T_{min})^{0.653}(\frac{T_{max} - T_{min}}{2} + 17.8)R_a \quad (1)$$

Where R_a defined as extraterrestrial radiation (MJ m^{-2} day^{-1}), computed using day data of the year and study area latitude given as 26.6639° S using $R_a = \frac{24\times60}{\pi} \times G_{SC} \times d_r \times [\omega_s sin(\phi)sin(\delta) + cos(\phi)cos(\delta)sin(\omega_s)]$. The parameter G_{SC} defined as a solar constant (0.0820 MJ m^{-2} min^{-1}), d_r as inverse relative Earth-Sun distance, ω_s as sunset hour angle (radians), ϕ as latitude (radians), δ as solar declination (radians). The coefficient in Equation 1 demonstrates an empirical basis, which is necessary for this implementation. After obtaining PET, the water balance is calculated using Equation 2.

$$D_i = P_i - PET_i \quad (2)$$

Further determined and handled null values in the computed PET_i and P_i by substituting null values and zeros with a constant small value, such as 0.01 to avoid undefined log-transform logarithmic operation. The two parameters were normalized using a $\log(x + 1)$ to stabilize the variance and reduce skewness [24].

$$SPEI_i = W_i - \frac{C_0 + C_1 W + C_2 W^2}{1 + d_1 W + d_2 W^2 + d_2 W^3} \quad (3)$$

$$W_i = \sqrt{-2ln(p)}\ if\ p \leq 0.5 \text{ OR } W_i = \sqrt{-2ln(1-p)}\ if\ p > 0.5 \quad (4)$$

$$C_0 = 2.5155, C_1 = 0.8028, C_2 = 0.0103, d_1 = 1.4328, d_2 = 0.1892, d_3 = 0.0013$$

Given W_i as shown in Equation 4, SPEI is then computed using Equation 3 on a temporal time scale (SPEI-3), calibration period, Gamma distribution index for standardization. The computed final SPEI values can then be classified as shown in **Table 2** for subsequent drought analysis:

Table 2. SPEI Characteristics [3, 10]

SPEI index	Classification
≥ 2	Extremely wet
$1.5 \sim 1.9$	Very wet
$1.0 \sim 1.49$	Moderate wetness
$0.99 \sim 0$	Mild wetness
$0 \sim -0.99$	Mild drought
$-1.00 \sim -1.49$	Moderate drought
$-1.5 \sim -1.9$	Severely drought
≤ -2	Extreme drought

Preprocessing and Training-Testing Data Partitioning:

The third phase focused on input features to the proposed predictive framework. These features include precipitation, PET, and water balance extracted from the dataset, while SPEI is defined as the target variable. All input features are normalized using MinMax scaling in the interval [0,1], to ensure feature comparability and numerical stability. A defined customized function transforms the datasets into a supervised time-series format, while a 3-month consecutive time step is utilized as the model input and SPEI values as predicted target at the subsequent time step. This phase produces a 3-D input element, which is suitable for sequence-based models, while the dataset was randomly partitioned into training and testing sets using 80:20 ratio split, with a fixed random state of 42, which guarantees reproducibility of this experiment setup.

Selected Machine Learning and Deep Learning Models:

This section presents ML and DL models used in this study; a brief discussion is made to reduce complexity and redundancy of the study. However, scholars are advised to visit the cited paper for in-depth understanding.

Random Forest

Random forest is a supervised ensemble ML that accumulates a large number of decisions trees and merges them to form a robust ensemble method [25], [26]. According to research scholars, RF has similar advantages as SVR when dealing with overfitting and uncertainty. However, RF constructs multiple modelling approaches for uncertainty and overfitting reduction. Ensemble based RF, regression tree, makes use of bagging technique for accuracy predictions using decision architectures. Using these large quantities of trees, is to allow the model to accommodate large data points, and interpretation can be easily archived [27]. The basic RF architecture requires the following: the number of regression trees and randomized input sample, where estimates are combined to make a single prediction. Moreover, this study used scikit-learn to invoke regression tasks, then create a regressor model, which consists of decision trees. The randomization function is used to ensure the recreatability of the model features and target value.

Support Vector Regression

SVR is an ML algorithm, which is an extension of SVM introduced to characterize various ML properties, namely, robust to outliers, managing high non-linear feature spaces, determining sparse solutions, which support vectors, regularizing, also flexible and non-linear to regression tasks for unseen data. The above-mentioned SVR characteristics allow SVR to have various advantages as compared to other ML algorithms, as it is prone to positive and negative classes, and less sensitive to overfitting, as it adopted SVM risk minimization structure. Hydrology forecasting is one of the successful fields in which this model is utilized, however, it was previously used for short- and long-term drought forecasts. For this study, "rbf" is used, and various previous scholars have demonstrated its effectiveness. Given a set of input data $x_i, x_j \in R^k$ where $i = 1,2, \dots, n$ is mapped to a higher non-linear dimensional feature space applied using Equation 5 [28]. [29], [30]:

$$\Phi(x_i, x_j) = exp(-\gamma||x_i - x_j||^2) \quad (5)$$

Where the model uses hyperparameters gamma (γ), epsilon (ε), and positive constant (C) to control model complexity and tolerance trade off, smoothness boundary decision, also give a specific margin of tolerance. Notably, SVR is not an ensemble ML algorithm, but rather a regression model with the capability to capture multi nonlinear patterns in sample data, while RF is an ensemble of multiple decision trees.

SVR-RF

In this study, a heterogeneous stacking model (SVR-RF) is constituted to leverage the strength of the two base ML models and ensure optimal forecast accuracy. Although these models are independently trained using the same data, the stacking model is computed by averaging the outputs of the individual models at the output level [31], [32].

Convolutional Neural Network

CNN, using feedforwarding as its primary neural network consisting of various layers that process fixed size input data for training characteristics. In cases where the input data is a dependent variable, the use of CNN is convenient because of calculation cost and overfitting address. In terms of time series, sound, and image input, CNN automatically employs a spatial hierarchy, which makes CNN a suitable algorithm for learning in this regard. [1], [13], [33]. This study employs a 1-D CNN to extract features from sequential input data by capturing local patterns and produce an effective representation, which can be understood by subsequent layers [34]. This layer contains various filters, which extract data from the input and convert it to a feature map. In this case, the convolutional layer is given by Equation 6 for each filter:

$$h_i^{(k)} = ReLU\left(\sum_{j=1}^{n} W_j^{(k)} \cdot x_{i+j-\left\lfloor\frac{n}{2}\right\rfloor} + b^{(k)}\right) \quad (1)$$

Where $k \in \{1,2,\dots, conv\_filetr\}$, n is the kernel size, $W_j^{(k)}$ denotes the kernel weight for k filters, $b^{(k)}$ the bias term, ReLU(z) is the maximum between the interval (0, z). The output shape of this layer for subsequent layers is given by $(B, T, conv\_filter)$. The second layer, which is the pooling layer extracts certain features from the output of the convolutional layer to produce matrices with low dimension, which are single values. In addition, the computational cost is reduced by this layer [1]. This is archived by the operation in Equation 7 where its output is $(B, T/2, conv\_filter)$ feed to the last layer the dropout layer, $\forall i \in \{0,1,\dots, T/(2-1)\}$:

$$y_i = max(h_{2i}, h_{2i+1}) \quad (2)$$

Long Short-Term Memory

The use of LSTM, a variant of RNN, in meteorological forecasting follows a substantial number of layers linked to a memory block for feature extraction of nonlinear attributes for the given input data. The feature extracting process stores the extracted data in the kernel memory. The first layer processes a sequence of inputs $X = (x_1, x_2, \dots, x_n)$ that return a complete sequence of unseen states $H = (h_1, h_2, \dots, h_n)$, then the formation of the three gates in the LSTM architecture are given as follows [24]:

$$\mathrm{f_t} = \sigma(\mathrm{W_f} \cdot [\mathrm{h_{t-1}}, \mathrm{x_t}] + \mathrm{b_f}) \quad (3)$$

$$\mathrm{i_t} = \sigma(\mathrm{W_i} \cdot [\mathrm{h_{t-1}}, \mathrm{x_t}] + \mathrm{b_i}) \quad (4)$$

$$\tilde{\mathrm{C}}_\mathrm{t} = \tanh(\mathrm{W_C} \cdot [\mathrm{h_{t-1}}, \mathrm{x_t}] + \mathrm{b_C}) \quad (5)$$

$$\mathrm{C_t} = \mathrm{f_t} \odot \mathrm{C_{t-1}} + \mathrm{i_t} \odot \tilde{\mathrm{C}}_\mathrm{t} \quad (6)$$

$$\mathrm{o_t} = \sigma(\mathrm{W_o} \cdot [\mathrm{h_{t-1}}, \mathrm{x_t}] + \mathrm{b_o}) \quad (7)$$

$$\mathrm{h_t} = \mathrm{o_t} \odot \tanh(\mathrm{C_t}) \quad (8)$$

Where Equation 9 denotes the forget gate, Equation 9 denotes the input gate, Equation 10 denotes candidate memory, update of cell state shown by Equation 11, output gate by Equation 12, Equation 13 denotes the hidden state, σ Sigmoid activation, $\odot$ Element-wise multiplication and learnable parameters, W_*, b_* [35]. Furthermore, the self-attention mechanism is activated by the outputs of H. During the second layer, the model utilizes the three gate mechanisms as in the first layer, however, the model inputs the results generated by the self-attention mechanism instead of X and

returns h_n. For in-depth reading, scholars can refer to [1], [4], [10]. This study identifies the temporal relationship within the given input.

Artificial Neural Network

As previously mentioned by Schultz *et al.* and Haupt *et al.* [36], [37], the atmosphere is a complex, uncertain, and nonlinear environment. ANN in this case, is a suitable neural network as its architectural functions and structure are inspired by the biological neural network. Following its robustness in studying the connection between I/O and result in the best optimal output from the highly sophisticated environment [1]. In this study, an elevated level characterizes and combines the output features obtained from LSTM and CNN, to make the final predictions, as this algorithm has strong capabilities to evolve output patterns. In a study by Akinci *et al.* [38] states that shallow learners are typically a good fit for output predictions given an input. ANN in this study is utilized as a shallow learner due to its model simplicity and consists of few layers to classify the output of the DL models, CNN and LSTM for distinct interpretable features.

The CNN-LSTM-ANN

Research shows that various scholars applied hybrid neural networks in various drought domains, particularly CNN-LSTM. Using different parameters, researchers predicted the SPEI characteristics according to **Table 2**. The use of this hybrid demonstrated that such models are really shaping the future forecasting [1], [10], [13], [39]. The proposed model consists of three neural networks, CNN, LSTM, and ANN. For the study CNN-1D is the primary phase of the hybrid, which features extract patterns and sequence from the input data using convolutional layer, which consists of 64 filters, ReLu activation, kernel size of 2 and a MaxPooling 1-D layer with pool size of 2 to reduce dimensionality. The extracted features are fed to a stacked LSTM to process the temporal pattern of the captured data discovered within the input data, using two LSTM layers where each consists of 50 memory units. The first LSTM layer returns a full sequence while the second LSTM layer returns the temporal representation. Lastly, ANN computes the final output by integrating the obtained extracted features from CNN and LSTM using two connected dense layers consisting of 64 and 32 neurons respectively. Scholars like Nyamane *et al*. [13] influenced the use of ANN in this study, as they discovered that ANN discovers hidden patterns and defines the data points relationship, with this augment, utilizing ANN in the proposed model output layer, gives better prediction proximity where the stacked interconnected nodes within the ANN structure discover patterns and relationships form CNN and LSTM output. This architecture hierarchy allows the proposed model to self-optimize using both temporal and spatial dependencies.

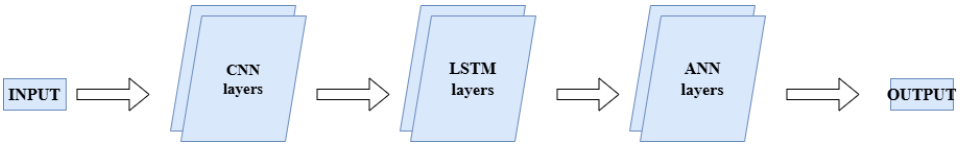

Figure 3. Proposed CNN-LSTM-ANN for meteorological drought prediction.

Hyperparameter configuration:

This section presents the hyperparameter configuration for the ML and DL models. **Table 3** shows the default hyperparameter used as baseline and hyperparameter values for optimization for model performance. The model selection represents various learning paradigms ranging from tree based, kernel base and DL models, enabling a comparative rigorous evaluation of regression performance.

Table 3. Hyperparameter configuration

	Model	Model Architecture Hyperparameter	Training hyperparameter
ML	RF	Input reshaping: Flattening (3D to 2D), Model type: RFR, Number of trees: 100, Random state: 42, Minimum samples for split: 2,	Training type: Batch ensemble training, Output: Continuous Regression Predictions

	Model	Model Architecture Hyperparameter	Training hyperparameter
		Minimum samples per leaf: 1, Maximum features per split: 1.0, Bootstrap sampling: True	
	SVR	Input reshaping: Flattening (3D to 2D), Model type: SVR, Kernel type: RBF, Regularization parameter C: 100, Kernel coefficient: 0.1, Epsilon insensitive loss: 0.1.	Training type: Batch training, Output: Continuous Valued Regression Predictions
	SVR-RF	Model type: Prediction Level Stacking, Stacking strategy: Simple Arithmetic Mean, Base learner: SVR and RF, Meta-learner: Rule Based Averaging, Fusion method: Unweighted Averaging	Training type: Independent training of base learners
DL	CNN	Model type: 1D CNN, Conv layer: 1, Conv Filter: 64, kernel size: 2, Activation function: ReLU, Input shape: 3D, Pooling type: MaxPooling1D, Pool size: 2, Dense layers: 2, Dense layer 1 neurons: 50, Dense layer 2 neurons: 25, Output layer neurons: 1, Output activation: Linear.	Optimizer: Adam, Learning rate: 0.001, Loss function: Mean Squared Error (MSE), Evaluation metric: Mean Absolute Error (MAE), Number of epochs: 50, Batch size: 16, Validation strategy: Hold-out validation using (X_test, y_test)
	LSTM	Model type: Stacked LSTM, LSTM layers: 2, LSTM Layer 1 units: 50, LSTM Layer 2 units: 50, Layer 1 return sequences: True, Layer 2 return sequences: False, Input shape: 3D, Hidden Dense layer neurons: 25, Hidden Dense layer activation: ReLU, Output layer neurons: 1, Output activation: Linear.	
	ANN	Input reshaping method: Flattening 2D transformation, Model type: Feedforward ANN, Hidden layers: 3, Hidden layer 1 neurons: 64, Hidden layer 2 neurons: 32, Hidden layer 3 neurons: 16, Activation function: ReLU, Output layer neurons: 1, Output activation: Linear, Weight initializer: Glorot Uniform, Bias initializer: Zeros	
	CNN-LSTM-ANN	Input shape: 3D, Conv Filter: 64, kernel size: 2, Activation function: ReLU, Pooling type: MaxPooling1D, Pool size: 2, LSTM Layer 1 units: 50, Layer 1 return sequences: True, LSTM Layer 2 units: 50, Dense layer 1 neurons: 64, Dense layer 1 activation: ReLU,	

Model	Model Architecture Hyperparameter	Training hyperparameter
	Dense layer 2 neurons: 32, Dense layer 2 activation: ReLU, Output layer neurons: 1, Output activation: Linear, Flatten layer: Used after LSTM.	

Evaluation Metrics:

This study focuses on mean squared error (MSE) and mean absolute error (MAE), which are statistical analysis matrices that are used to measure the accuracy of the proposed models: SVR, RF, CNN, ANN, LSTM, SVR-RF, CNN-LSTM, CNN-LSTM-ANN performances. However, the low MAE value observed indicates that the similarities between observed and predicted values are high, whereas low MSE indicates that predicted and observed values are closer to each other. These metrics are used to evaluate metrological drought parameters (Maximum and Minimum Temperature, Precipitation). The given equations, F_i, O_i, n are defined as forecast data, observed value, and number of observed cycles, respectively. **Table 4** outlines the metrics description.

Table 4. Evaluation Metrics

Metrics	Description	Equation
MAE [5, 10, 13]	The accuracy is determined by the difference between the observed and forecasted	$MAE = \frac{\sum_{i=1}^{n} \lvert F_i - O_i \rvert}{n}$
MSE [7, 40, 41]	The squared difference of the observed and forecasted values	$MSE = \frac{\sum_{i=1}^{n} (F_i - O_i)^2}{n}$
Correlation coefficient [42]	Estimates how closely the observed matches and forecasted values	$r^2 = \frac{\sum_{i=1}^{n} [(O_I - \overline{O_I})(F_I - \overline{F_I})]}{\sqrt{\sum_{i=1}^{n} (O_I - \overline{O_I})^2} \sqrt{\sum_{i=1}^{n} (F_I - \overline{F_I})^2}}$

3. Result

Experiment settings

This experiment was conducted using open-source tools, systems with specific software and hardware. The hardware setup includes an HP Envy x360 2-in-1 laptop 15, running on Windows 11 Enterprise version 23H2, powered by an AMD Ryzen 7 7730U with Radeon Graphics 2.00 GHz processor and 16GB of RAM. The hardware configuration includes a high-performance system with a multi-core processor, a large RAM, and GPU support for training and tuning ML and DL models. The software includes python 3.10.12, executed using Jupyter Notebook version 6.5.7 and an online repository Kaggle environment with key libraries, such as climate-indices, Matplotlib, Pandas, amongst others. The parameters, which are used in the proposed CNN-LSTM-ANN and SVR-RF models are shown **Table 3**, for the prediction of drought using meteorological data. To evaluate the performance of the proposed model, **Table 4** was applied to the results obtained.

SPEI Estimation

Computing SPEI for 3-months, from the obtain data, was initiated by performing exploratory data analysis, upon completion, a discovery that was made is that; the obtained data consisted of null values. However, to avoid negative influence on the proposed model, we obtain 8060 data points after performing EDA, which are used to compute PET and water balance, the results are shown in **Figure 4** respectively. PET computation uses maximum and minimum

temperatures variables; followed by a detailed computational by making utilizing Equation 1 to obtain the daily PET for the period 2013 to 2024. In addition, the calculated PET and the precipitation obtained were used to determine the water balance (water distribution over time) aggregated by Equation 2, which defined the wetness or dryness of the earth surface.

Comparing the distribution of PET and the water balance over time. A visual observation is made from **Figure 4a** that past the year 2021, the plot exhibits a significant clustered fluctuation density of the PET value from 10 – 16 mm/day, which demonstrates intense temporal resolutions, this is the climatic conditions influenced by rapid change in temperature, humidity. Moreover, the distribution of water balance D_i over time shows fluctuation that follows a similar trend as PET suggesting an inverse proportionality relationship. Most values float below zero, which gives an indication that PET exceeds precipitation.

Table 5. Statistical Analysis

	Water balance	**PET**	**Prcp**	**SPEI**
Count	8060.00	8060.00	8060.00	8060.00
Mean	-7.979908	0.000180	0.000085	-0.555095
STD	7.926967	1.000058	1.000110	1.020447
Min	-17.303103	-3.339319	-0.385595	-3.090000
25%	-12.234725	-0.736611	-0.385595	-1.169358
50%	-10.016210	-0.008942	-0.385595	-0.730944
75%	-7.266953	0.778806	-0.224539	-0.131855
Max	87.451227	2.773067	13.230988	3.090000

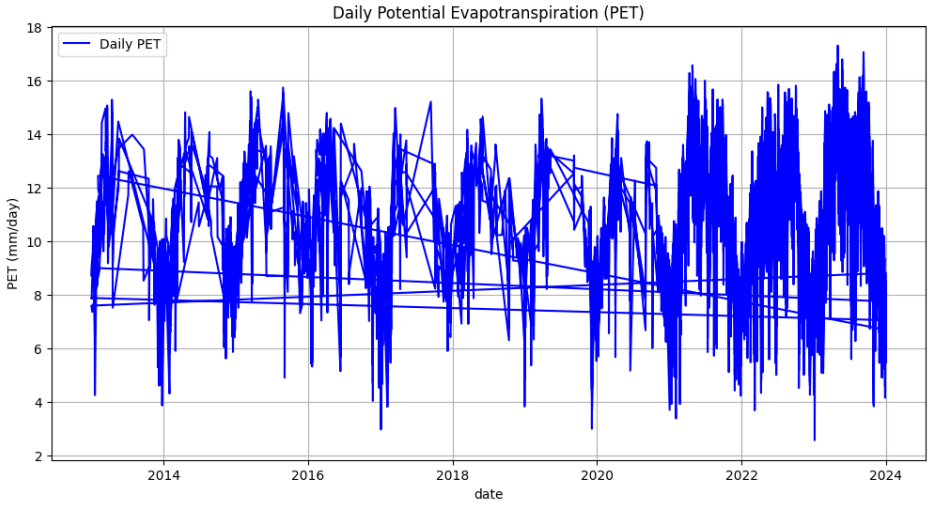

(a)

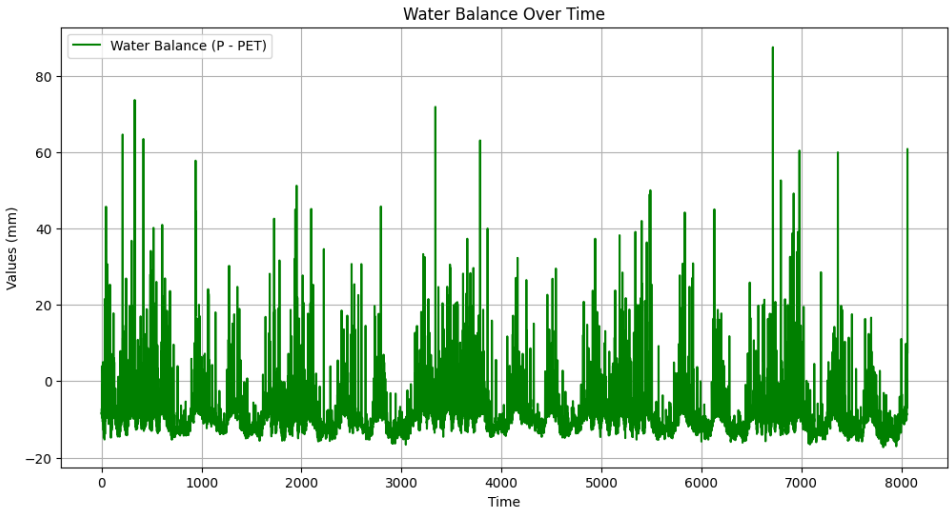

(b)

Figure 4. (a) Daily potential evapotranspiration (PET) and (b) Water balance over the study period.

This explains why during the evaporation process, the atmosphere capacity to volatize earth water was higher than the normal rainfall over that period, leading to the depiction of water and resulting in drought conditions. Similarly, in the statistical analysis of precipitation in **Table 5**, the mean value of PET exceeds precipitation, suggesting the lack of consistency of rainfall over a time interval. This analysis is further observed through the water balance IQR (Q3-Q1) approximately 5.0 demonstrating a shortfall trend, while the precipitation max of 13.23 demonstrated a high skewness with Q3 of -0.22.

SPEI is evaluated by water balance and PET for temporal scale three, with SPEI ranges from -3 to 3. Positive SPEI indicates wet conditions, while negative SPEIs denote dry conditions. **Figure 5** demonstrates an overlaid horizontal distribution, which shows different drought severities (see **Table 2**). A cluster of common prolonged negative values is noticeably exhibited, indicating intense dry conditions. However, it is evident that occasionally extreme drought occurs, marked by the spikes dropping to -3. The frequently transitioning spikes, particularly between severe and moderate levels, suggest water resource vulnerability. Moreover, SPEI values are normalized and standardized using the gamma distribution transformation.

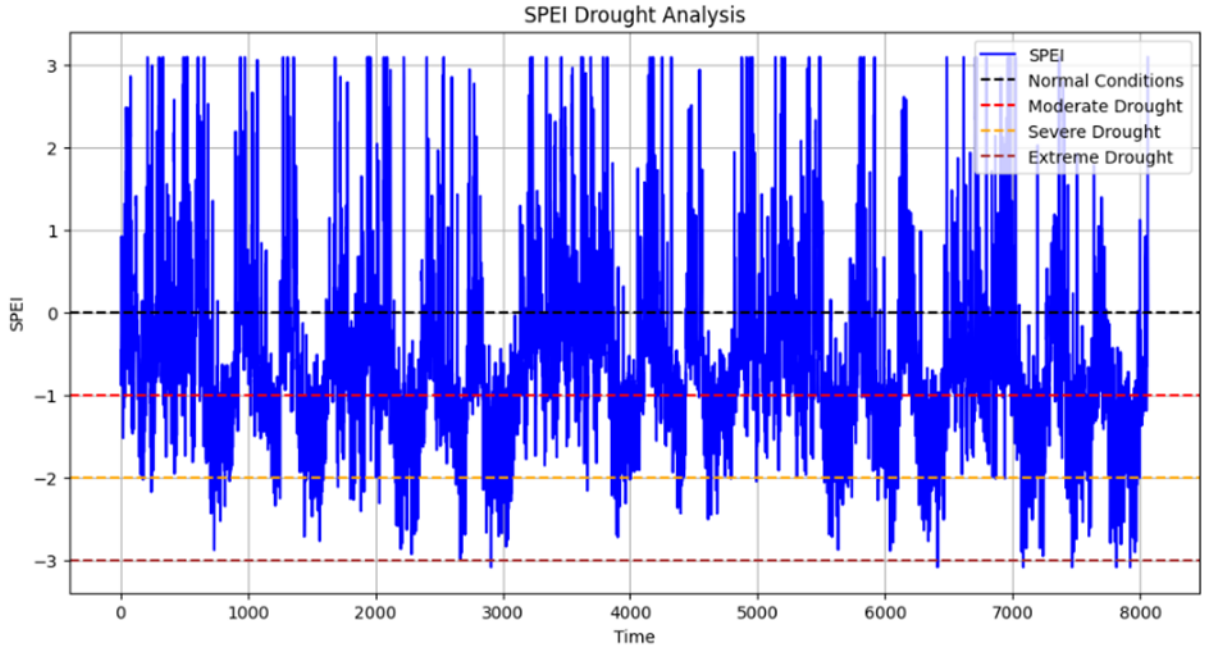

Figure 5. SPEI drought analysis of the study area

Ensemble ML and DL Estimations:

In this sub-section, 3 DL and two ensemble ML are used to predict drought severity in the study area using meteorological data. However, we obtained PET, water balance and SPEI, which were not included in the dataset, these parameters are used in the proposed models. These parameters (PET, water balance and Prcp) are used as input features, while the target variable, SPEI was calculated. These parameters used in SPEI computation utilized a timescale of 3 months to generate the results obtained. In addition, the probabilistic distribution fit, shown in Equation 4, results in indefinite probabilistic. Moreover, for training and assessing the learning algorithms, the data sets were divided into 80% training data and 20% testing data over 50 epochs. To assess the proposed modes effectiveness for SPEI drought forecasting, standalone models CNN, LSTM, ANN, SVR, RF, and hybrid CNN-LSTM are utilized as benchmarking models. These models used in research extensively make them an ideal effective baseline model for evaluating proposed architecture. The results indicate that the predicted SPEI using CNN, LSTM, ANN and CNN-LSTM over a time interval, most prediction spikes range between $(0, \sim -1.5)$.

Further comparison and analysis of each model performance **Table 6**, which gives the different statistical results of MAE, MSE and correlation coefficient for proposed algorithms. The overall performance of these models demonstrates that the algorithms succeeded in making drought predictions with varying accuracy. Among DL models, Table 6 shows that ANN outperformed other DL algorithms, evident with the low MSE of 0.2640 with a high correlation coefficient (r^2) of 0.7416. This result demonstrates superior accuracy and variance description within the DL paradigm. However, CNN and LSTM demonstrate comparable results with MSE values of 0.2674 and 0.2735, respectively, with a consistent r^2 value approximately 0.73, showing capturing spatio-temporal drought capabilities. The hybrids models did not exhibit competitive performance compared to standalone models. Contrary to DL models, SVR achieved desirable results obtaining the highest r^2 of 0.8590 and low MAE of 0.3415 demonstrating strong predictive capabilities among ML models. Moreover, synthesizing SVR and RF by combining tree-base and kernel base learners shows improvements in SPEI-3 prediction archiving low MSE of 0.2776 and competitive r^2 of 0.8558. This suggests that combining both SVR and RF approaches reduces the error rate better than the stand-alone algorithms. RF is the least performing model from the three ML model obtaining the lowest r^2 of 0.8435 and high MAE of 0.3858, this marks RF the underperformed algorithm for ensemble ML models. The overall performance of

the learning paradigms across all the performance metrics indicates that ML model outperforms DL model for SPEI-3 predictions, highlights the precision of ML based frameworks for meteorological drought predictions in this study

Table 6. Performance of models for drought prediction evaluated using MSE, MAE, r^2

Learning Paradigm	Models	MSE	MAE	r^2
DL	CNN	0.2674	0.3686	0.7383
	LSTM	0.2735	0.3481	0.7323
	ANN	0.2640	0.3555	0.7416
	CNN-LSTM	0.2699	0.3569	0.7358
	CNN-LSTM-ANN	0.2699	0.3677	0.7358
ML	SVR	0.2839	0.3415	0.8590
	RF	0.2956	0.3858	0.8435
	SVR-RF	0.2776	0.3549	0.8558

Figure 6 demonstrates a comparative comparison between benchmarking algorithms and the proposed hybrid based on the actual and predicted SPEI, where this figure consists of five graphs of different DL models. Each plot shows the predicted SPEI (in distinct colours) and the actual SPEI in a blue colour for visual observation on how the predicted SPEI tracks the actual SPEI. Figure 6a shows how CNN model successfully captured local variability and SPEI-3 fluctuations given its conventional architectural feature extraction. However, temporal data extracted by CNN, which represents a local pattern shows difficulties in identifying temporal dependencies. The predicted SPEI demonstrates a fluctuation trend with underestimations compared to the actual SPEI showing a significant prediction deviation. This observation interprets CNN's correlation coefficient in Table 6. We learned that LSTM is a more reliable algorithm in capturing and processing sequential data than CNN. Figure 6b demonstrates an improved temporal proportion in capturing SPEI-3 with valley and peaks closer to the true SPEI capturing temporal trends compared to CNN. Similarly to CNN, underestimated are observed. Figure 6c exhibits ANN, a shallow learner that demonstrates coherent visual overlaps in the predicted SPEI-3 compared to CNN and LSTM. Frequency and magnitude of the SPEI-3 fluctuation are preserved by ANN shown nonlinear regression capabilities. This observation is consistent with the qualitative results shown in Table 6, ANN achieving low MSE and high r^2 compared to the other DL model. CNN-LSTM hybrids use both algorithms feature extraction and sequential learning techniques to make predictions, the figure shows the best fit than of individual algorithms with smooth and aligned to the true. Moreover, the proposed hybrid CNN-LSTM-ANN model exhibits to be the best fit model to the actual SPEI, balancing feature extraction and sequential architecture with a redefined ANN prediction. The hybrid shows dispersed predicted SPEI variability compared to the actual SPEI, with tracking of both spikes demonstrating high amplitude peaks. This observation corresponds with the high MAE of 0.3667 in **Table 6**, showing that the model error rate slightly higher that of CNN-LSTM. The general observation from **Figure 6e** shows the complexity of drought predictions through the variability and noise observed in the models, providing a competitive assessment on the strength and constraints of the hybrid and single DL architecture in drought predictions.

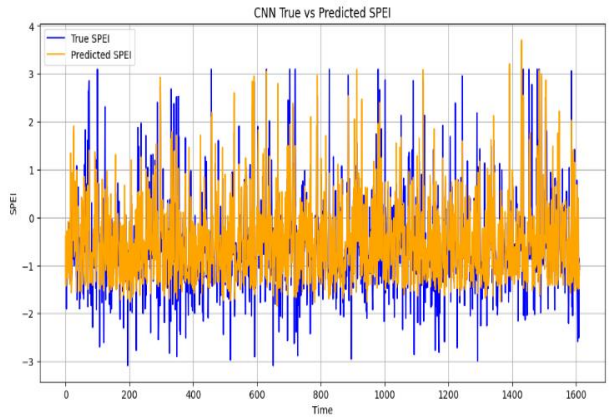

(a)

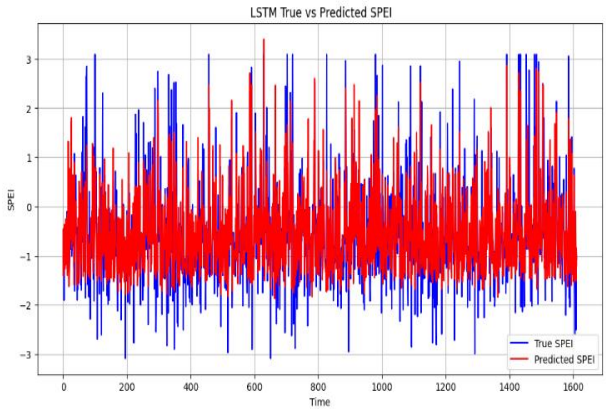

(b)

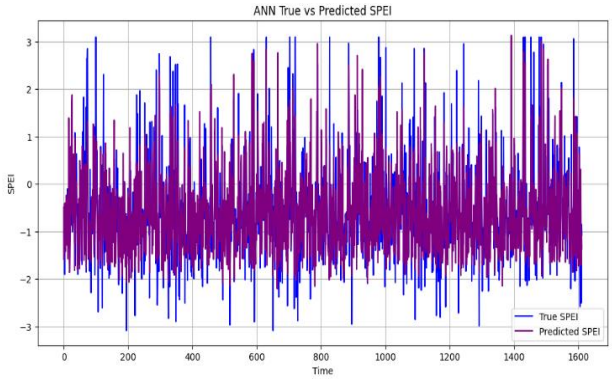

(c)

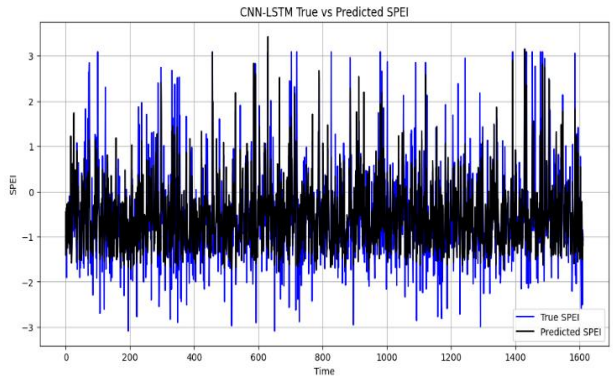

(d)

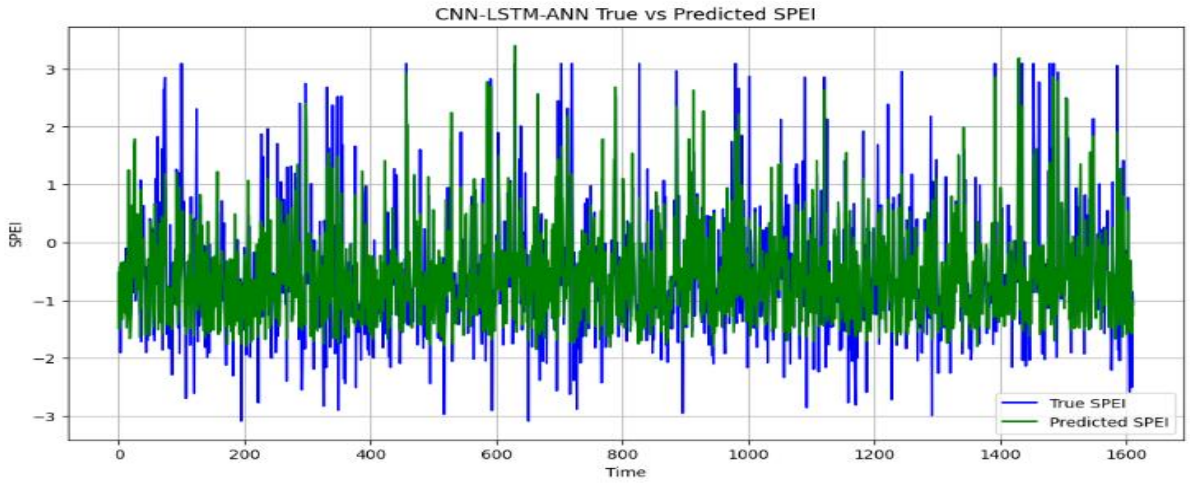

(e)

Figure 6. Comparison of true and DL model predicted SPEI values.

Discussion

Monitoring droughts is an especially important activity in climate change. Research shows that various tools are being utilized to combat drought characterization in arid regions. These tools include drought indices, remote sensing, statistical tests, and ML and DL algorithms utilized to collect, analyze, and monitor data patterns [3]. The results of this research paper on medium range meteorological drought forecast using SPEI-3 were calculated using historical meteorological data for the North West province, South Africa. The data included Temperature (average, minimum, maximum), Precipitation, amongst others, required for drought evaluation. This study proposed ML algorithms SVR, RF, and three neural networks: CNN, LSTM, ANN to predict meteorological drought. The results of this study demonstrate a correlation between the calculated SPEI and the proposed models with an MSE ranging from 0.2640 to 0.2956 for both ML and DL algorithms (see **Table 6** and **Figure 6**), with an MAE range of 0.3415 to 0.3858. The results obtained show an erratic distribution of drought events, varying across the DL algorithms in terms of SPEI-3, with CNN, LSTM, ANN CNN-LSTM, CNN-LSTM-ANN showing promising results during the training and testing phase of the simulations acquiring an average MAE and MSE training 0.3581 and 0.2661 respectively. During the testing phase, the evaluation metrics MAE and MSE recorded an average of 0.3593 and 0.2689, respectively, with an average r^2 of 0.7368. Using **Table 6**, a scatter plot shown in **Figure 7** was generated, where each model is represented. The x-axis represents the MAE, which explains how the predicted value deviates from the true value, whereas the y-axis represents the MSE, the square difference between the true and predicted values. **Figure 7** shows that ANN is the algorithm that performed most with a least squared error of 0.2640. However, proposed SVR with an absolute error of 0.3415, making it the best model in terms of MAE. RF model is the worst performing model in both metrics with the largest error predictions. **Figure 7** further demonstrates that the DL models are closely clustered below 0.275 MSE and between 0.35 and 0.37, demonstrating similarities within in the models, while ML models are scattered above 0.275.

In comparison with existing forecasting models, En-Nagre *et al.* [3], used climate data to assess meteorological drought using ML algorithms. The results show high accuracy predictions for SPEI-3 and 12 and irregular drought distribution with negative trend patterns. Similarly, Yalçın *et al.* [10] proposed a hybrid CNN and LSTM approach to estimate SPEI in Turkey, the results show the proposed CNN-LSTM model outperformed the benchmarking DL model for SPEI-12 compared to other timescales. Mehr *et al.* [1], also proposed hybrid CNN-LSTM, with GP, ANN, LSTM, CNN as benchmarking algorithms. The study results show the hybrid outperformed benchmarking algorithms in drought predictions with MAE for SPEI-3 during the training and testing phase ANN (0.53), CNN (0.52), LSTM (0.53), CNN-LSTM (0.46) and ANN (0.71), CNN (0.65), LSTM (0.64), CNN-LSTM (0.60), respectively. In comparison with Table 6 of this study, the proposed framework outperformed Mehr *et al.* [1] proposed model on SPEI-3. Yalcin *et al.* [10] in four provinces in Türkiye, shows that CNN-LSTM with 0.13, 0.04, 0.02, 0.008 MAE with an r^2 of approximately 0.99 outperforms the proposed models in **Table 6**. Similar argument can be made with the study by Nyamane *et al.* [13] the superior metrices performance suggests that this study models underperformed in predicting meteorological drought conditions. Moreover, Kombo *et al.* [43] proposed EEMD-SVR-RF to predict groundwater in Rugarama (Mukaange) at various day leading time. The results for 15, 30, 60, 90-days' time show an MAE of 0.0624 (0.0022), 0.0539(0.0014), 0.0344(0.0011), and 0.0382(0.0012). The models' r^2 ranges between 0.86 – 0.96 demonstrating close rations between observed and forecasted. These values surpass the r^2 values of this study, as shown in **Table 6.** A summarised comparison is tabled in **Table 7**.

Table 7. Comparison with similar existing studies

Ref	Model	SPEI	MSE	MAE	CC
[13]	CNN-LSTM	3	-	0.082513	0.913167
[4]	RF	3	0.14	0.31	-
[44]	RF	3	-	0.39	0.74
	ANN-MLP		-	0.64	0.35
[3]	RF	3	-	0.45	0.96

Ref	Model	SPEI	MSE	MAE	CC
[39]	LSTM	3	-	0.024	0.992
[45]	SVR	3	-	0.103	0.973
Proposed model	SVR-RF	3	0.2776	0.3549	0.8558
	CNN-LSTM-ANN	3	0.2699	0.3677	0.7358

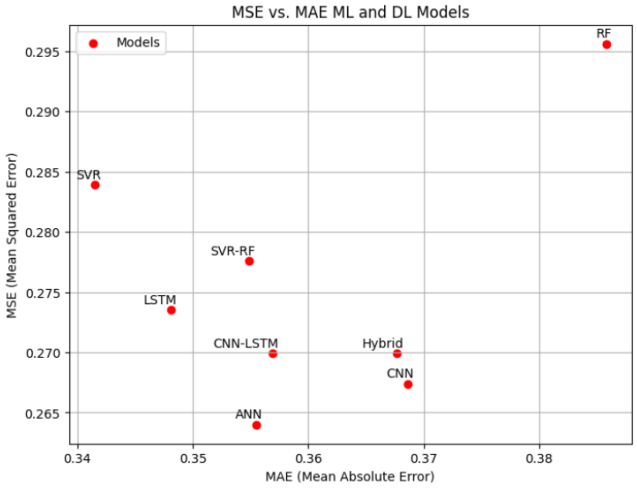

Figure 7. Scatter plot of MSE versus MAE for all tested models.

4. Conclusion

In closing, this study focuses on improving drought prediction approaches in the North West Province of South Africa, which has experienced significant impact on wildlife, agriculture and socioeconomic challenges due to drought occurrence in this region. This research employs ensemble ML, DL and SPEI, a drought index to examine drought events for 10 years using temperature, precipitation identified as crucial parameters that influence drought. The performance of the model's was assessed using evaluation matrices, such as MAE, MSE, and r^2. The results obtained show an erratic distribution of drought events, varying between the DL and ML algorithms in terms of SPEI-3, with ANN achieving a least squared error rate of 0.2640 and SVR achieving an absolute error of 0.3415. The practical implications of this study extend to various sectors, including government policymakers, climate and environmental planning, water resource management, and agricultural sector. This is a specific region focused study aimed at improving drought monitoring systems using ML and DL models for stakeholders tailing to address meteorological drought in the region. This study encountered various limitations including the scarcity of meteorological data, where reliable, accessible and frequent gaps were observed in the dataset, which posed a significant constraint to this study, as a more consistent and compressive data is critical to provide more depth insight into then factors influencing meteorological drought. In future research, exploring other temporal scales and meteorological parameters to enhancing the accuracy of drought forecasting can be achieved.

References:

[1] A. Danandeh Mehr, A. Rikhtehgar Ghiasi, Z. M. Yaseen, A. U. Sorman, and L. Abualigah, "A novel intelligent deep learning predictive model for meteorological drought forecasting," *Journal of Ambient Intelligence and Humanized Computing*, vol. 14, no. 8, pp. 10441-10455, 2023, doi: 10.1007/s12652-022-03701-7.

[2] J.-L. Zhang, X.-M. Huang, and Y.-Z. Sun, "Multiscale spatiotemporal meteorological drought prediction: A deep learning approach," *Advances in Climate Change Research*, vol. 15, no. 2, pp. 211-221, 2024, doi: 10.1016/j.accre.2024.04.003.

[3] K. En-Nagre *et al.*, "Assessment and prediction of meteorological drought using machine learning algorithms and climate data," *Climate Risk Management*, vol. 45, p. 100630, 2024/01/01/ 2024, doi: https://doi.org/10.1016/j.crm.2024.100630.

[4] A. Mokhtar *et al.*, "Estimation of SPEI meteorological drought using machine learning algorithms," *IEEe Access*, vol. 9, pp. 65503-65523, 2021, doi: 10.1109/ACCESS.2021.3074305.

[5] H. Qian, W. Wang, and G. Chen, "Assessing forecast performance of daily reference evapotranspiration: A comparison of equations, machine and deep learning using weather forecasts," *Journal of Hydrology*, vol. 644, p. 132101, 2024, doi: 10.1016/j.jhydrol.2024.132101.

[6] X. Zhong *et al.*, "FuXi-ENS: A machine learning model for medium-range ensemble weather forecasting," *arXiv preprint arXiv:2405.05925*, vol. 3, 2024, doi: 10.48550/arXiv.2405.05925.

[7] C. B. Pande *et al.*, "Forecasting of meteorological drought using ensemble and machine learning models," *Environmental Sciences Europe*, vol. 36, no. 1, p. 160, 2024/09/11 2024, doi: 10.1186/s12302-024-00975-w.

[8] X. Li, Z. Li, W. Huang, and P. Zhou, "Performance of statistical and machine learning ensembles for daily temperature downscaling," *Theoretical and Applied Climatology*, vol. 140, no. 1, pp. 571-588, 2020/04/01 2020, doi: 10.1007/s00704-020-03098-3.

[9] L. Olivetti and G. Messori, "Advances and prospects of deep learning for medium-range extreme weather forecasting," *Geosci. Model Dev.*, vol. 17, no. 6, pp. 2347-2358, 2024, doi: 10.5194/gmd-17-2347-2024.

[10] S. Yalçın, M. Eşit, and Ö. Çoban, "A new deep learning method for meteorological drought estimation based-on standard precipitation evapotranspiration index," *Engineering Applications of Artificial Intelligence*, vol. 124, p. 106550, 2023, doi: 10.1016/j.engappai.2023.106550.

[11] U. W. Humphries, M. Waqas, P. T. Hliang, P. Dechpichai, and A. Wangwongchai, "A deep learning perspective on meteorological droughts prediction in the Mun River Basin, Thailand," *AIP Advances*, Article vol. 14, no. 8, 2024, Art no. 085026, doi: 10.1063/5.0209709.

[12] P. Hewage, M. Trovati, E. Pereira, and A. Behera, "Deep learning-based effective fine-grained weather forecasting model," *Pattern Analysis and Applications*, vol. 24, no. 1, pp. 343-366, 2021/02/01 2021, doi: 10.1007/s10044-020-00898-1.

[13] S. Nyamane, M. A. M. Abd Elbasit, and I. C. Obagbuwa, "Harnessing Deep Learning for Meteorological Drought Forecasts in the Northern Cape, South Africa," *International Journal of Intelligent Systems*, vol. 2024, no. 1, p. 7562587, 2024, doi: https://doi.org/10.1155/2024/7562587.

[14] M. Ehteram, M. Afshari Nia, F. Panahi, and A. Farrokhi, "Read-First LSTM model: A new variant of long short term memory neural network for predicting solar radiation data," *Energy Conversion and Management*, vol. 305, p. 118267, 2024/04/01/ 2024, doi: https://doi.org/10.1016/j.enconman.2024.118267.

[15] M. Mukhtar *et al.*, "Development and Comparison of Two Novel Hybrid Neural Network Models for Hourly Solar Radiation Prediction," *Applied Sciences*, vol. 12, no. 3, p. 1435 doi: 10.3390/app12031435.

[16] O. Bamisile *et al.*, "Comprehensive assessment, review, and comparison of AI models for solar irradiance prediction based on different time/estimation intervals," *Scientific Reports*, vol. 12, no. 1, p. 9644, 2022/06/10 2022, doi: 10.1038/s41598-022-13652-w.

[17] D. Escobar-González *et al.*, "Soil Moisture Forecast Using Transfer Learning: An Application in the High Tropical Andes," *Water*, vol. 16, no. 6, p. 832 doi: 10.3390/w16060832.

[18] T. E. o. E. Britannica. "North West Province, South Africa." https://www.britannica.com/place/North-West-province-South-Africa (accessed 12 Jan, 2025).

[19] L. G. C. C. S. Program. "The North West province is in the process of updating its climate change strategy." https://letsrespondtoolkit.org/municipalities/north-west/ (accessed 15 January 2025).

[20] P. s. Weather. "North West farmers continue to lose animals due to drought." https://www.peoplesweather.com/news/north-west-farmers-continue-to-lose-animals-due-to-drought-53/ (accessed 14 January 2025).

[21] P. Tau. "Farmers desperate for help as drought devastates large parts of SA." City Press. https://www.news24.com/citypress/news/farmers-desperate-for-help-as-drought-devastates-large-parts-of-sa-20191113 (accessed 14 January, 2025).

[22] M. Achite, O. M. Katipoglu, S. Şenocak, N. Elshaboury, O. Bazrafshan, and H. Y. Dalkılıç, "Modeling of meteorological, agricultural, and hydrological droughts in semi-arid environments with various machine learning and discrete wavelet transform," *Theoretical and Applied Climatology*, vol. 154, no. 1, pp. 413-451, 2023/10/01 2023, doi: 10.1007/s00704-023-04564-4.

[23] D. Althoff, R. A. d. Santos, H. C. Bazame, F. F. d. Cunha, and R. Filgueiras, "Improvement of Hargreaves–Samani reference evapotranspiration estimates with local calibration," *Water*, vol. 11, no. 11, p. 2272, 2019, doi: 10.3390/w11112272.

[24] H. A. Afan *et al.*, "LSTM Model Integrated Remote Sensing Data for Drought Prediction: A Study on Climate Change Impacts on Water Availability in the Arid Region," *Water*, vol. 16, no. 19, p. 2799 doi: 10.3390/w16192799.

[25] A. J. Hill, R. S. Schumacher, and I. L. Jirak, "A New Paradigm for Medium-Range Severe Weather Forecasts: Probabilistic Random Forest–Based Predictions," (in English), *Weather and Forecasting*, vol. 38, no. 2, pp. 251-272, 01 Feb. 2023 2023, doi: https://doi.org/10.1175/WAF-D-22-0143.1.

[26] A. Elbeltagi *et al.*, "Prediction of meteorological drought and standardized precipitation index based on the random forest (RF), random tree (RT), and Gaussian process regression (GPR) models," *Environmental Science and Pollution Research*, vol. 30, no. 15, pp. 43183-43202, 2023/03/01 2023, doi: 10.1007/s11356-023-25221-3.

[27] M. Ali, R. Prasad, Y. Xiang, M. Jamei, and Z. M. Yaseen, "Ensemble robust local mean decomposition integrated with random forest for short-term significant wave height forecasting," *Renewable Energy*, vol. 205, pp. 731-746, 2023/03/01/ 2023, doi: https://doi.org/10.1016/j.renene.2023.01.108.

[28] K. F. Fung, Y. F. Huang, and C. H. Koo, "Coupling fuzzy–SVR and boosting–SVR models with wavelet decomposition for meteorological drought prediction," *Environmental Earth Sciences*, vol. 78, no. 24, p. 693, 2019/12/04 2019, doi: 10.1007/s12665-019-8700-7.

[29] J. Piri, M. Abdolahipour, and B. Keshtegar, "Advanced Machine Learning Model for Prediction of Drought Indices using Hybrid SVR-RSM," *Water Resources Management*, vol. 37, no. 2, pp. 683-712, 2023/01/01 2023, doi: 10.1007/s11269-022-03395-8.

[30] K. F. Fung, Y. F. Huang, C. H. Koo, and M. Mirzaei, "Improved SVR machine learning models for agricultural drought prediction at downstream of Langat River Basin, Malaysia," *Journal of Water and Climate Change*, vol. 11, no. 4, pp. 1383-1398, 2019, doi: 10.2166/wcc.2019.295.

[31] Z. Tan, J. Zhang, Y. He, Y. Zhang, G. Xiong, and Y. Liu, "Short-Term Load Forecasting Based on Integration of SVR and Stacking," *IEEE Access*, vol. 8, pp. 227719-227728, 2020, doi: 10.1109/ACCESS.2020.3041779.

[32] S. Kumar, M. Srivastava, and V. Prakash, "Enhancing Mutual Fund Price Prediction: A Hybrid Ensemble Approach with Random Forest, SVR, Ridge, and Gradient Boosting Regressors," in *International Conference on Signal, Machines, Automation, and Algorithm*, 2023: Springer, pp. 551-566.

[33] J. Long, C. Xu, Y. Wang, and J. Zhang, "From meteorological to agricultural drought: Propagation time and influencing factors over diverse underlying surfaces based on CNN-LSTM model," *Ecological Informatics*, vol. 82, p. 102681, 2024/09/01/ 2024, doi: https://doi.org/10.1016/j.ecoinf.2024.102681.

[34] A. Gujar, T. Gupta, and S. Roy, "Hybrid Model for Impact Analysis of Climate Change on Droughts in Indian Region," in *Lecture Notes in Computer Science (including subseries Lecture Notes in Artificial Intelligence and Lecture Notes in Bioinformatics)*, 2024, vol. 14505 LNCS, pp. 227-242, doi: 10.1007/978-3-031-53969-5_18.

[35] A. B. Abbes, R. Inoubli, M. Rhif, and I. R. Farah, "Combining deep learning methods and multi-resolution analysis for drought forecasting modeling," *Earth Science Informatics*, vol. 16, no. 2, pp. 1811-1820, 2023/06/01 2023, doi: 10.1007/s12145-023-01009-4.

[36] M. G. Schultz *et al.*, "Can deep learning beat numerical weather prediction?," *Philosophical Transactions of the Royal Society A: Mathematical, Physical and Engineering Sciences*, vol. 379, no. 2194, 2021, doi: 10.1098/rsta.2020.0097.

[37] S. E. Haupt, P. A. Jiménez, J. A. Lee, and B. Kosović, "1 - Principles of meteorology and numerical weather prediction," in *Renewable Energy Forecasting*, G. Kariniotakis Ed.: Woodhead Publishing, 2017, pp. 3-28.

[38] T. C. Akinci, O. Topsakal, and M. I. Akbas, "Machine Learning Methods from Shallow Learning to Deep Learning," in *Shallow Learning vs. Deep Learning: A Practical Guide for Machine Learning Solutions*: Springer, 2024, pp. 1-28.

[39] A. Dikshit, B. Pradhan, and A. Huete, "An improved SPEI drought forecasting approach using the long short-term memory neural network," *Journal of Environmental Management*, vol. 283, p. 111979, 2021/04/01/ 2021, doi: https://doi.org/10.1016/j.jenvman.2021.111979.

[40] H. Citakoglu and Ö. Coşkun, "Comparison of hybrid machine learning methods for the prediction of short-term meteorological droughts of Sakarya Meteorological Station in Turkey," *Environmental Science and Pollution Research*, vol. 29, no. 50, pp. 75487-75511, 2022/10/01 2022, doi: 10.1007/s11356-022-21083-3.

[41] D. Markovics and M. J. Mayer, "Comparison of machine learning methods for photovoltaic power forecasting based on numerical weather prediction," *Renewable and Sustainable Energy Reviews*, vol. 161, p. 112364, 2022/06/01/ 2022, doi: https://doi.org/10.1016/j.rser.2022.112364.

[42] F. Ghobadi and D. Kang, "Multi-Step Ahead Probabilistic Forecasting of Daily Streamflow Using Bayesian Deep Learning: A Multiple Case Study," *Water*, vol. 14, no. 22, p. 3672 doi: 10.3390/w14223672.

[43] O. H. Kombo, S. Kumaran, E. Ndashimye, and A. Bovim, "An Ensemble Mode Decomposition Combined with SVR-RF Model for Prediction of Groundwater Level: The Case of Eastern Rwandan Aquifers," in *Computer Science On-line Conference*, 2022: Springer, pp. 312-328.

[44] E. Harsányi, "Predicting agricultural drought in central Europe by using machine learning algorithms," *Journal of Agriculture and Food Research*, vol. 20, p. 101783, 2025/04/01/ 2025, doi: https://doi.org/10.1016/j.jafr.2025.101783.

[45] K. F. Fung, Y. F. Huang, and C. H. Koo, "Improvement of SVR-Based Drought Forecasting Models using Wavelet Pre-Processing Technique," *E3S Web Conf.*, 10.1051/e3sconf/20186507007 vol. 65, // 2018. [Online]. Available: https://doi.org/10.1051/e3sconf/20186507007.